한국복합신소재구조학회 논문집 제4권, 제1호, 2013년 03월
J. Korean Soc. Adv. Comp. Struc. Vol. 4, No. 1, pp. 9-14, March 2013
DOI http://dx.doi.org/10.11004/kosacs.2013.4.1.009

ISSN 2093-5145(Print)
ISSN 2288-0232(Online)

복합소재 기둥 구조의 적층배열 변화에 따른 고유진동 및 모드 특성

김규동[1] · Guillermo Rus[2]· 이상열[3]

안동대학교 토목공학과 석사과정[1] · 스페인 국립 Granada 대학교 구조공학과 교수[2]
안동대학교 토목공학과 조교수[3]

Natural Frequency and Mode Characteristics of Composite Pole Structures for Different Layup Sequences

Kim, Gyu-Dong[1] · Rus, Guillermo[2] · Lee, Sang-Youl[3]

[1]Master Student, Department of Civil Engineering, Andong National University, Andong, Korea
[2]Professor, Department of Structural Mechanics, University of Granada, Granada, Spain
[3]Assistant Professor, Department of Civil Engineering, Andong National University, Andong, Korea

Abstract: The dynamic analysis of poles made of advanced composite materials is carried out for different length-thickness ratios and layup sequences. The numerical results using ABAQUS obtained for plates and shells are in good agreement with those reported by other investigators. The new results for laminated composite pole structures in this study mainly show the effect of the interactions between the radius-length ratio and other various parameters. The effect of fiber angles of long composite poles also investigated. Key observation points are discussed and a brief design guideline is given.

Key Words: Composites, Layup sequences, Finite element analysis, Free vibration

1. Introduction

With the advancement of technology in composite materials, applications of laminated composites to pole structures are advantageous because of their light weight, high specific stiffnesses and high specific strengths. However, laminated poles with a long length may result in a significant change of the dynamic characteristics during various external loading. Therefore, it is essential to study the effect of fiber angles and geometries simultaneously on the frequency of layered poles. The mechanical behaviors of a structure depend on the properties of the fibers and the matrix and in the amount and orientations of the fibers.

Numerous theories exist for laminated composite plates or structures. Many these theories were developed originally for thin shells and are based on the Kirchhoff-Love kinematic hypothesis (Sanders, 1963). However, these classical theories are inadequate to describe accurately the kinematic behavior of anisotropic composite shells. The first-order shear deformation theory (FSDT) has been extended by other investigators to deal with those problems (Kraus, 1967; Sanders, 1059; Zukas and Vinson, 1971). In general, a first order shear deformation theory can describe easily and accurately the kinematic behavior of a thin composite structure (Reddy, 2004). The composite pole types can be practically applied to wind turbine towers. Polyzois et al. (2009) studied static and dynamic characteristics of multi-cell jointed glass fiber-reinforced polymer (GFRP) wind turbine towers.

주요어: 복합소재, 적층배열, 유한요소 해석, 고유 진동

Corresponding author: Lee, Sang-Youl
Department of Civil Engineering, Andong National University, 388 Songchon-dong, Andong, Kyoungsangbuk-do 760-749, South Korea
Tel: +82-54-820-5847, E-mail: lsy@andong.ac.kr

투고일: 2013년 1월 4일 / 수정일: 2013년 1월 24일 / 게재확정일: 2013년 2월 14일

In this paper, we performed a finite element analysis based on FSDT to analyze the free vibration of laminated poles with a long length. Very little research has been studied to identify the interaction between vibrations and layup sequences for long composite pole type structures. The length-thickness ratio and layup sequence of laminated poles with different geometries could play a dominant role in determining and efficiently controlling the dynamic characteristics of the composite structure without causing a change in its material properties. Numerical examples are focused on the changes in natural frequencies for different radius-length ratios, layup sequences, shapes of the cross-section and interactions between these parameters.

2. Basic Theory

In the laminated structures, the stiffness properties are function of the normal coordinate. In Fig. 1 a cross-section of laminated plate composed of N layers is presented. A linear elastic properties of the anisotropic layers are characterized by the tensor of elasticity C_{ijkl} .In many applications, it can be as sumed that calculations of shell stiffness properties can be performed neglecting the differences in spa-tial and shell mid-surface metrics. In this case, the Hook's law for each layer can be written by

$$S_{ij} = C_{ijkl} E_{kl} \tag{1}$$

Since the present formulation is based on the natural coordinate reference frame, we introduce here an explicit transformation scheme between natural coordinates and the global coordinate system, to obtain a natural coordinate based constitutive equation. The stress tensor in the natural coordinate can be written as follows:

$$\tilde{S}_{ij} = \tilde{C}_{ijkl} \tilde{E}_{kl} = \tilde{J}_0 \mathbf{T} \tilde{D}_{ijkl} \mathbf{T}^{\mathbf{T}} \tilde{E}_{kl} \tag{2}$$

where $\tilde{J}_0$ is the determinant of the Jacobian matrix and is the $\tilde{D}_{ijkl}$ constitutive matrix for orthotropic materials with the material angle θ .The transformation matrix in Eq. 2 is given $\mathbf{T}$ by Han et al. (2004). The strain energy U can be expressed by

$$U = \frac{1}{2} \int_A \int_{-h/2}^{h/2} \tilde{C}_{ijkl} \tilde{E}_{ij} \tilde{E}_{kl} \, d\xi_3 \, dA \tag{3}$$

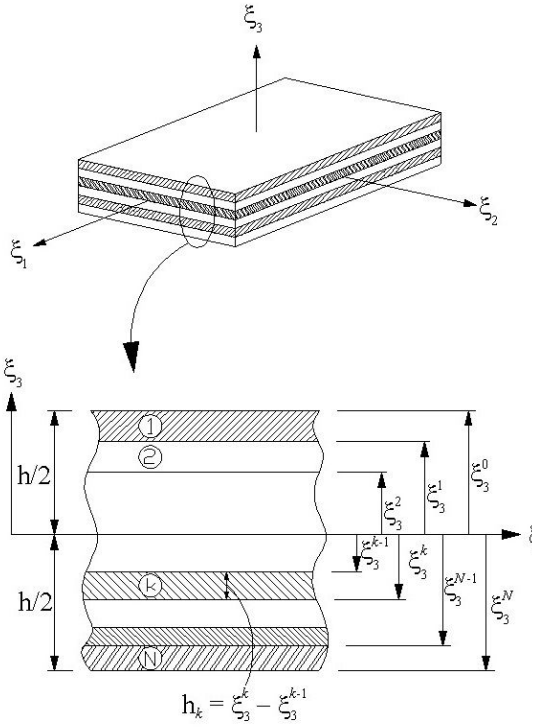

Fig. 1 Cross-section of laminated plate composed of N layers.stress resultants and couples and laminated shell stiffness characteristics

After integration, throughout the thickness, the strain energy can be obtained in terms of shell quantities:

$$A_{\alpha\beta\gamma\delta}, B_{\alpha\beta\gamma\delta}, D_{\alpha\beta\gamma\delta} = \int_{-h/2}^{h/2} \tilde{C}_{\alpha\beta\gamma\delta} (1, \xi_3, \xi_3^2) \, d\xi_3$$
$$A_{\alpha 3 \beta 3} = k_s \int_{-h/2}^{h/2} \tilde{C}_{\alpha 3 \beta 3} \, d\xi_3 \tag{4}$$

The Reissner's value of 5/6 is used as the transverse shear correction factor in the FE formulation based on the first shear deformation theory.

The shell element displays resultant forces acting on a laminate which are obtained by integration of stresses through the laminate thickness. In this study, we impose the plane state on the natural constitutive equation of Eq. 2 before forming the equivalent constitutive equation. The constitutive relations of the composite laminate are as follows:

$$\begin{Bmatrix} N_{\alpha\beta} \\ M_{\alpha\beta} \\ Q_{\alpha 3} \end{Bmatrix} = \begin{bmatrix} A_{\alpha\beta\gamma\delta} & B_{\alpha\beta\gamma\delta} & 0 \\ B_{\alpha\beta\gamma\delta} & D_{\alpha\beta\gamma\delta} & 0 \\ 0 & 0 & A_{\alpha 3\beta 3} \end{bmatrix} \begin{Bmatrix} \tilde{E}^{m}_{\gamma\delta} \\ \tilde{E}^{b}_{\gamma\delta} \\ \tilde{E}^{s}_{\beta 3} \end{Bmatrix} \quad (5)$$

3. Finite element model

In the current study, the ABAQUS program was used to develop finite element models for simulating the structural behavior of laminated composite poles. The poles tested had an average height of 5.00 m from the base. The sectional properties are shown in Fig. 2. Each ply of the laminates has equal thickness. The material properties of the plies are E1=40.0E2, G12=0.5E2, G23=0.6E2 G13=0.5E2, and Poisson's ratio=0.25. The produced natural frequencies in this study are normalized. Fig. 3 shows finite element laminated composite models using different cross-section types in ABAQUS program. The arrangement of the fibers in a pole structure is governed by the structural requirements and by the process used to fabricate the part. The mass density is assumed for convenience to have a unit value. The boundary conditions are free-clamped supported such as a cantilever beam. Fig. 4 shows the whole finite element modelling of pole structures using ABAQUS.

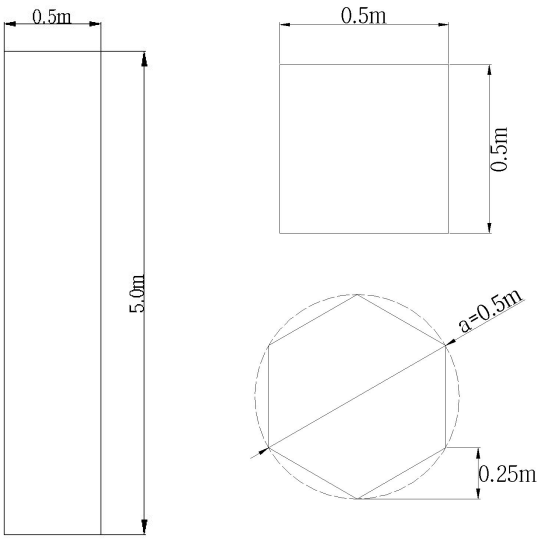

(a) Longitudinal-section (b) Cross-section

Fig. 2 Two type test models

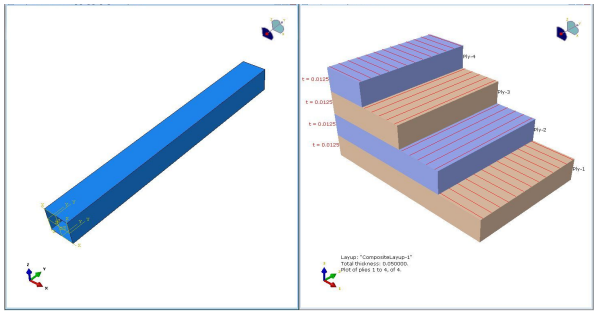

(a) Quadrangle shape

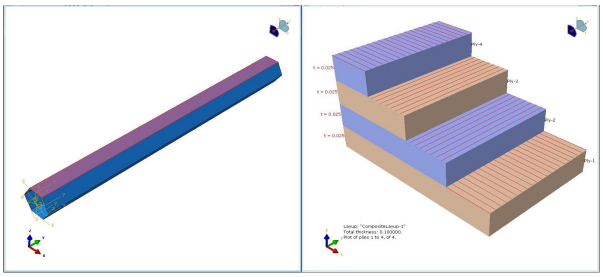

(b) Hexagon shape

Fig. 3 ABAQUS modeling of laminated composites.

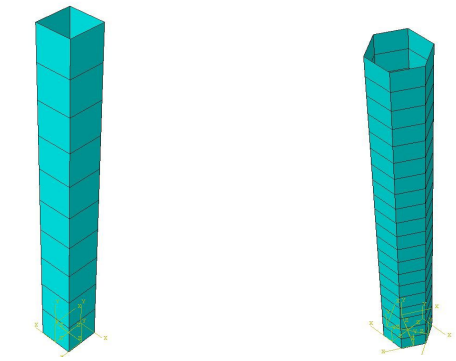

(a) Quadrangle model (b) Hexagon model

Fig. 4 ABAQUS modeling of two types.

4. Numerical examples

4.1 Quadrangle poles

Table 1~3 show non-dimensional natural frequencies of quadrangle poles for different layup sequences and length-thickness ratios (a/h). It can be observed from the tables that the use of different layup sequences (symmetry or anti-symmetry) has a negligible effect on the laminated poles, regardless of the fiber angles and length-thickness ratios. On the other hand, the induced frequency for the same layup sequence is strongly dependent on the fiber angle, especially for [0/90]s and $[15/-75]_2$.

Table 1. Non-dimensional natural frequencies for different layup sequences (quadrangle, a/h=5.0)

Mode	Symmetry layup sequence				
	[0/90]s	[15/-75]s	[30/-60]s	[45/-45]s	[60/-30]s
Ⅰ	0.239	0.158	0.108	0.096	0.108
Ⅱ	0.537	0.617	0.672	0.604	0.673
Ⅲ	0.954	0.888	0.850	1.201	0.852
Ⅳ	1.634	1.875	1.852	1.718	1.856
Mode	Anti-symmetry layup sequence				
	$[0/90]_2$	$[15/-75]_2$	$[30/-60]_2$	$[45/-45]_2$	$[60/-30]_2$
Ⅰ	0.230	0.153	0.106	0.095	0.109
Ⅱ	0.537	0.615	0.661	0.600	0.676
Ⅲ	0.930	0.868	0.850	1.194	0.841
Ⅳ	1.634	1.872	1.825	1.707	1.858

Table 2. Non-dimensional natural frequencies for different layup sequences (quadrangle, a/h=10.0)

Mode	Symmetry layup sequence				
	[0/90]s	[15/-75]s	[30/-60]s	[45/-45]s	[60/-30]s
Ⅰ	0.476	0.311	0.214	0.190	0.213
Ⅱ	1.062	1.203	1.327	1.195	1.324
Ⅲ	1.886	1.752	1.679	2.398	1.683
Ⅳ	3.235	3.660	3.651	3.397	3.645
Mode	Anti-symmetry layup sequence				
	$[0/90]_2$	$[15/-75]_2$	$[30/-60]_2$	$[45/-45]_2$	$[60/-30]_2$
Ⅰ	0.466	0.306	0.211	0.189	0.215
Ⅱ	1.062	1.204	1.310	1.191	1.331
Ⅲ	1.856	1.724	1.683	2.389	1.667
Ⅳ	3.234	3.661	3.612	3.384	3.656

Table 3. Non-dimensional natural frequencies for different layup sequences (quadrangle, a/h=50.0)

Mode	Symmetry layup sequence				
	[0/90]s	[15/-75]s	[30/-60]s	[45/-45]s	[60/-30]s
Ⅰ	0.951	0.619	0.425	0.377	0.424
Ⅱ	2.116	2.377	2.634	2.375	2.628
Ⅲ	3.754	3.481	3.325	4.786	3.332
Ⅳ	6.441	7.227	7.243	6.746	7.225
Mode	Anti-symmetry layup sequence				
	$[0/90]_2$	$[15/-75]_2$	$[30/-60]_2$	$[45/-45]_2$	$[60/-30]_2$
Ⅰ	0.941	0.613	0.421	0.377	0.426
Ⅱ	2.116	2.379	2.614	2.371	2.639
Ⅲ	3.721	3.450	3.335	4.776	3.312
Ⅳ	6.440	7.235	7.195	6.734	7.250

Table 4. Non-dimensional natural frequencies for different layup sequences (hexagon, a/h=5.0)

Mode	Symmetry layup sequence				
	[0/90]s	[15/-75]s	[30/-60]s	[45/-45]s	[60/-30]s
Ⅰ	0.215	0.139	0.094	0.083	0.095
Ⅱ	0.585	0.667	0.582	0.521	0.586
Ⅲ	0.896	0.791	0.896	1.197	0.898
Ⅳ	1.761	1.911	1.585	1.459	1.595
Mode	Anti-symmetry layup sequence				
	$[0/90]_2$	$[15/-75]_2$	$[30/-60]_2$	$[45/-45]_2$	$[60/-30]_2$
Ⅰ	0.205	0.134	0.093	0.083	0.095
Ⅱ	0.585	0.666	0.572	0.517	0.586
Ⅲ	0.868	0.770	0.897	1.191	0.887
Ⅳ	1.761	1.877	1.561	1.447	1.593

Table 5. Non-dimensional natural frequencies for different layup sequences (hexagon, a/h=10.0)

Mode	Symmetry layup sequence				
	[0/90]s	[15/-75]s	[30/-60]s	[45/-45]s	[60/-30]s
Ⅰ	0.428	0.274	0.186	0.165	0.187
Ⅱ	1.161	1.305	1.150	1.032	1.152
Ⅲ	1.774	1.559	1.773	2.392	1.777
Ⅳ	3.497	3.755	3.131	2.891	3.139
Mode	Anti-symmetry layup sequence				
	$[0/90]_2$	$[15/-75]_2$	$[30/-60]_2$	$[45/-45]_2$	$[60/-30]_2$
Ⅰ	0.417	0.268	0.184	0.164	0.187
Ⅱ	1.161	1.306	1.135	1.026	1.154
Ⅲ	1.739	1.529	1.778	2.382	1.761
Ⅳ	3.497	3.699	3.095	2.875	3.139

Table 6. Non-dimensional natural frequencies for different layup sequences (hexagon, a/h=50.0)

Mode	Symmetry layup sequence				
	[0/90]s	[15/-75]s	[30/-60]s	[45/-45]s	[60/-30]s
Ⅰ	0.855	0.543	0.370	0.329	0.371
Ⅱ	2.315	2.585	2.283	2.053	2.287
Ⅲ	3.530	3.096	3.521	4.774	3.528
Ⅳ	6.972	7.451	6.220	5.754	6.231
Mode	Anti-symmetry layup sequence				
	$[0/90]_2$	$[15/-75]_2$	$[30/-60]_2$	$[45/-45]_2$	$[60/-30]_2$
Ⅰ	0.844	0.537	0.367	0.328	0.371
Ⅱ	2.315	2.588	2.266	2.046	2.289
Ⅲ	3.492	3.062	3.531	4.761	3.507
Ⅳ	6.972	7.381	6.178	5.732	6.230

4.2 Hexagon poles

Table 4~6 show non-dimensional natural frequencies of hexagon poles for different layup sequences and length-thickness ratios (a/h). The produced natural frequencies for hexagon poles show a similar trend with those of quadrangle poles. The highest frequency occurs for the laminate with a layup sequence of [0/90/90/0] or [0/90/0/90] because its stiffness is greater than that of the others. The differences between the layup sequences for different fiber angles depend on many geometrical parameters such as shape of the cross-section, length-to-thickness ratio, and boundary conditions.

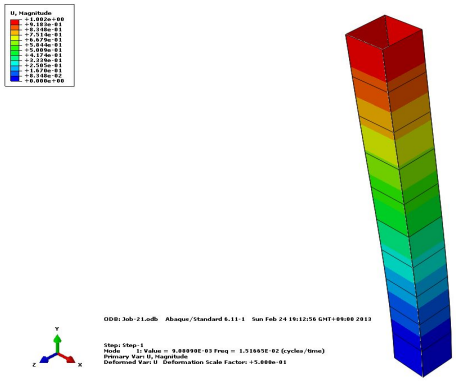

(a) Mode I

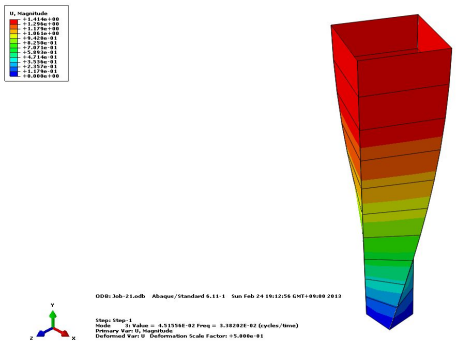

(b) Mode II

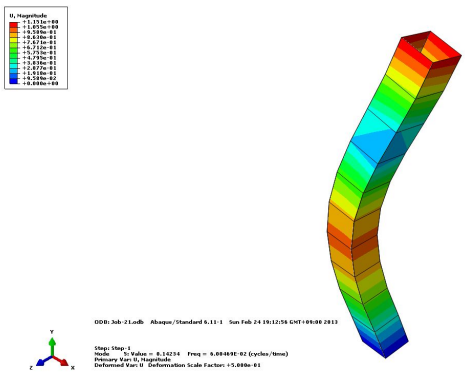

(c) Mode III

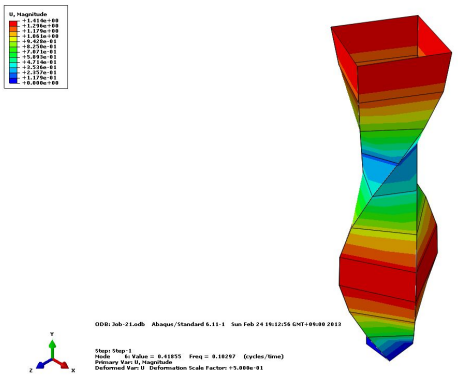

(d) Mode IV

Fig. 5 Mode shapes of quadrangle laminated composite poles (0/90/90/0).

4.3 Mode shapes

Figs. 5~6 show the mode shapes of symmetric cross-ply laminated quadrangle and hexagon poles with free-clamped ends. Each figure represents (a) symmetric vertical bending, (b) symmetric horizontal bending, (c) torsional, and (d) antisymmetric horizontal bending modes, respectively. As shown in the figures, some peculiar and complex mode shapes are produced due to the combined effect of both shapes of the cross-section of and layup stacking sequences.

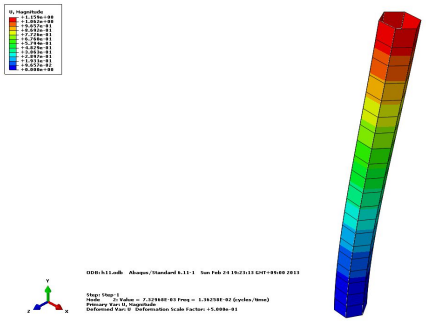

(a) Mode I

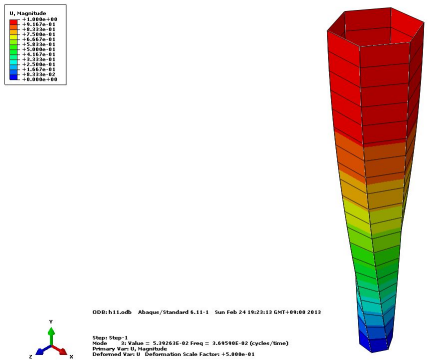

(b) Mode II

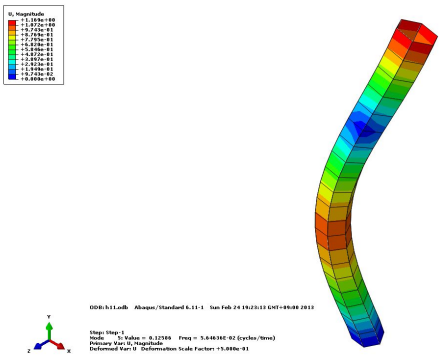

(c) Mode III

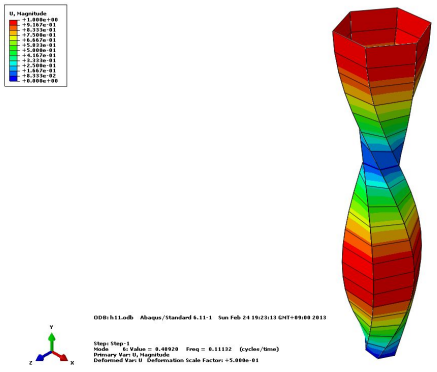

(d) Mode IV

Fig. 6 Mode shapes of hexagon laminated composite poles (0/90/90/0).

5. Summary and Conclusion

A technique based on the first-order shear deformation plate theory is developed to analyze the static and free vibration behavior of pole structures made of laminated composite materials. The usage of composite for poles could be an attractive approach from the practical point of view, not only because it has high stiffness but also because we can avoid the undesirable corrosion occurred in steel structures.

The technique is then implemented for quadrangle and hexagon poles of various layup sequences and end conditions to compare the results obtained from different length-to-thickness ratios. It is observed that the use of different layup sequences make little difference regardless of fiber angles, but the produced frequencies for different fiber angles become significant for various length-to-thickness ratios.

For composite poles with the closed section, e.g., quadrangle or hexagon box, the significance could be greater, because it is not only the properties of the materials but also the sectional properties of the member that makes large contributions to the overall behavior of the structure. The results of this study may serve as a benchmark for future guidelines in designing composite pole structures. But our parametric study is only an example and more studies should be carried out for individual design cases.

감사의 글

본 연구는 국토해양부 건설기술연구사업 연구비 지원(과제번호: 12CCTI-B063597-01, 10MW급 강재 및 3MW급 복합 합성구조 풍력발전타워 설계기술 개발)에 의해 수행되었음.

References

Dimos, J. P., Ioannis, G. R., and Nibong, U. (2009). “Static and dynamic characteristics of multi-cell jointed GFRP wind turbine towers.” *Comp. Struct.*, Vol. 90, pp. 34-42.

Han, S. C., Kim, K. D., Kanok-Nukulchai, W. (2004). “An element-based 9-node resultant shell element for large deformation analysis of laminated composite plates and shells.” *Struct. Eng. Mech.*, Vol. 18, No. 6, pp. 807-829.

Kraus, H. (1967). Thin elastic shells, Willy, New York.

Reddy, J. N. (2004). Mechanics of Laminated Composite Plates and Shells: Theory and Analysis, CRC Press, New York.

Sanders, J. L. Jr. (1959). An improved first approximation theory of thin shells, NASA TR-R24.

Sanders, J. L. Jr. (1963). “Nonlinear theories for thin shells Q.” *App. Math.*, Vol. 21, pp. 21-36.

Zukas, J. A. and Vinson, J. R. (1971). “Laminated transversely isotropic cylindrical shells.” *J. App. Mech.*, Vol. 38, pp. 400-407.